Original Article

Protective effect of high-affinity liposomes encapsulating astaxanthin against corneal disorder in the *in vivo* rat dry eye disease model

Tatsuharu Shimokawa,[1,2] Tatsuya Fukuta,[1] Toshio Inagi[1] and Kentaro Kogure[1,*]

[1]Department of Pharmaceutical Health Chemistry, Graduate School of Biomedical Sciences, Tokushima University Graduate School, 1 Shomachi, Tokushima 770-8505, Japan
[2]Fuji Research Laboratories Pharmaceutical Division, Kowa Company, Ltd., 332-1, Ohnoshinden, Shizuoka 417-8650, Japan

(Received 28 October, 2019; Accepted 11 December, 2019; Published online 6 March, 2020)

Oxidative stress induced by decreases in tear volume and excessive tear evaporation is a key factor in dry eye disease (DED). Previously, we reported that desiccation stress induces reactive oxygen species generation and up-regulated expression of age-related markers such as p53, p21 and p16. We also showed that the antioxidant astaxanthin prepared as a liposomal formulation could suppress these phenomena in the *in vitro* DED model. In this study, we evaluated the protective effect of liposomes encapsulating astaxanthin against superficial punctate keratopathy (SPK) in the *in vivo* rat DED model. This model of DED was characterized by decreased tear volume and increased fluorescein score as an indicator of SPK as well as upregulated expression of age-related markers. Repeat-dose of liposomal astaxanthin prevented increases in the fluorescein score and up-regulation of age-related markers. Liposomes bearing a slight positive surface charge had superior effects and higher affinity compared to neutral liposomes. Furthermore, fluorescence intensities in rat corneal epithelium after administration of high-affinity liposomes labeled with fluorescent dye were higher than those for neutral liposomes. In conclusion, we developed the high-affinity liposomal formulation that can prevent DED and promote antioxidative effects of astaxanthin.

***Key Words*: dry eye disease, oxidative stress, age-related markers, astaxanthin, liposomes**

Oxidative stress induced by decreases in tear volume and excessive tear evaporation is thought to be a key factor of dry eye disease (DED) which is a multifactorial disease that has a high rate of incidence worldwide.[1–3] A number of reports indicated a contribution of oxidative stress to disease pathology in an *in vitro* DED model using normal human corneal epithelial cells (HCECs) and in *in vivo* DED models using various animals.[4–11] These reports demonstrated that oxidative stress induces a generation of reactive oxygen species (ROS) that results in the production of several oxidative stress markers such as 8-hydroxy-2'-deoxyguanosine (8-OHdG), malondialdehyde (MDA), 4-hydroxy-2-nonenal (4-HNE) or hexanoyl-lysine (HEL), and increases in apoptosis via peroxidation of cell membranes and mitochondria dysfunction.[4–11] These studies also suggested that several substances that have antioxidant activity, such as the green tea polyphenol epigallocatechin gallate, *camellia japonica*, selenoprotein P, edaravone and omega-3 essential fatty acids, can improve corneal disorders.[6–11] Moreover, ROS generated by oxidative stress was shown to be an important factor in DED pathogenesis and antioxidants could thus be potential candidates for DED therapy.

Aging processes are also likely involved in DED given that the prevalence of DED increases with age. Lots of reports showed that the evaporation rate of tear film and DED phenotype are affected by factors such as age. These factors should thus be considered in clinical practice and likely have significant implications for management of DED, including the selection of appropriate topical medications.[2,11–14] Furthermore, many aging processes involve oxidative stress, and oxidative stress theory is recognized as a major aging process.[15,16] Aging processes often encompass the activation of the p53/p21 pathway and p16, the expression of which is induced by various endogenous and exogenous stressors, and is followed by inhibition of cyclin dependent kinase (Cdk) 2 and 4/6, respectively. Together these events lead to cell cycle arrest.[17–19]

Based on these reports, we hypothesized that oxidative stress may induce up-regulation of expression of age-related markers such as p53, p21 and p16, and antioxidants may represent potential candidates for treatment of DED via inhibition of ROS generation. Previously, we demonstrated that desiccation stress induces ROS generation and up-regulation of expression of age-related markers, such as p53, p21 and p16. Moreover, we previously evaluated the effect of the liposomal formulation of the antioxidant astaxanthin (Asx, Fig. 1), a carotenoid that is a common red pigment found in algae, fish and birds, and is widely used as a nutritional supplement and cosmetic ingredient,[20,21] on the age-related markers. Regarding antioxidative function of Asx, it has been reported that Asx can protect skeletal muscle from oxidative damage during exercise *in vivo*.[22] In our previous report, the liposomal formulation of Asx could suppress these phenomena in the *in vitro* DED model using HCECs.[23] We also demonstrated that liposomes comprising both neutral and cationic lipids that bore a slight positive charge exerted superior antioxidative effects compared to liposomes consisting of only neutral lipids. The positive surface charge is predicted to increase affinity of the liposomes for cell membranes, and thus high affinity, positively-charged liposomes should be advantageous for corneal treatments involving eye drops that typically exhibit low bioavailability due to the drainage system associated with tear flow.[23]

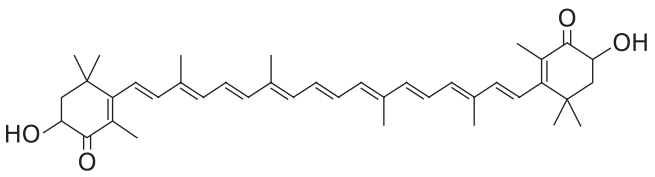

Fig. 1. Chemical structure of astaxanthin.

*To whom correspondence should be addressed.
E-mail: kogure@tokushima-u.ac.jp

doi: 10.3164/jcbn.19-102

In this study we expanded on our earlier findings by using the *in vivo* rat DED model to clarify the relationship between superficial punctate keratopathy (SPK), which is a major symptom of DED,[24–26] and the behavior of age-related markers. We also verified the correlation of findings for the *in vivo* rat DED model with those reported previously for the *in vitro* DED model. Subsequently, we evaluated the potential of high affinity liposomal formulations encapsulating Asx to exert a protective effect against SPK using the *in vivo* rat DED model.

Materials and Methods

Materials. Male Sprague-Dawley rats were purchased from Japan SLC, Inc. (Shizuoka, Japan). Sevoflurane was obtained from Mylan Pharmaceutical Co., Ltd. (Tokyo, Japan). Pentobarbital sodium was purchased from Kyoritsu Seiyaku Corporation (Somnopentyl; Tokyo, Japan). Phenol red-impregnated cotton threads (ZONE-QUICK) were obtained from the AYUMI Pharmaceutical Corporation (Tokyo, Japan). RNAlater RNA Stabilization Reagent and RNeasy Plus Mini kit were purchased from Qiagen GmbH (Hilden, Germany). Takara BioMasher Standard (Sterile), PrimeScript RT Master Mix (Perfect Real Time) and SYBR Premix Ex Taq II (Tli RNaseH Plus) were obtained from Takara Bio (Otsu, Japan). Egg phosphatidylcholine (EPC) was purchased from Sigma-Aldrich (St. Louis, MO). 1,2-Dioleoyl-3-trimethylammonium-propane chloride (DOTAP) was obtained from the NOF Corporation (Tokyo, Japan). Astaxanthin was purchased from FUJIFILM Wako Pure Chemical Corporation (Osaka, Japan). 1,1'-Dioctadecyl-3,3,3',3'-tetramethylindocarbocyanine perchlorate (DiI) was obtained from Invitrogen (Carlsbad, CA). All other reagents were of the highest grade commercially available.

The *in vivo* rat DED model. All animal experiments were conducted in compliance with a protocol that was reviewed and approved by the Institutional Animal Care and Use Committee of Fuji Research Laboratory of Kowa Company. Rats were kept under specific pathogen-free conditions for constant periods of 12 h light and 12 h dark. Environmental conditions were 23 ± 3°C and 50 ± 20% relative humidity, and the rats were allowed access to food and water *ad libitum*.

The commonly used *in vivo* rat DED model was prepared according to a previous study.[27] The exorbital lacrimal glands were surgically removed from the rats under inhalational anesthesia with sevoflurane, and the animals were then maintained for 14 to 25 days under the abovementioned conditions. On the same day, a sham operation was also carried out to prepare the control animals. On day 0, tear production volume and fluorescein score of rats were measured as described below and measurements were taken every 5 days until day 25.

Evaluation of tear production volume and fluorescein score. To measure tear production volume and fluorescein score, the rats were intraperitoneally anesthetized with pentobarbital sodium. The tear production volume was measured using phenol red-impregnated cotton threads (ZONE-QUICK) that are typically used in clinical practice. ZONE-QUICK threads were inserted into the lower eyelid and the length of color in the thread caused by tear wetting was measured three minutes later to determine the tear production volume.

We used fluorescein score methods to evaluate the SPK as a corneal epithelial disorder. [5,7–9,11,24–26] Fluorescein sodium solution (5 μl of a 2% solution), which can penetrate into damaged corneal epithelial cells, was dropped onto corneas from the abovementioned rats, and excess fluorescein solution was washed out with saline. Images of corneal surfaces were taken using a stereoscopic microscope with a LED light operating at 505 nm in a dark room. The corneas in the photographs were divided into 9 areas and each area was scored from 0 to 3 points depending on the density of fluorescein-stained areas. Fluorescein scores were calculated by totaling the points for the 9 areas.

Total RNA extraction from rat corneas and real-time PCR analysis. DED and control rats were euthanized by exsanguination under sevoflurane inhalation anesthesia. The eyeballs were removed and the corneas were resected. The corneas were immediately placed into 500 μl of RNA later RNA Stabilization Reagent and stored at –20°C. Total RNA was isolated from the corneas using a Takara BioMasher Standard (Sterile) and an RNeasy Plus Mini kit according to the manufacturer's protocol. The total RNA concentration was quantified using a Nanodrop 8000 (Thermo Scientific, Wilmington, DE). Thereafter, cDNA was synthesized from 25 ng of total RNA using PrimeScript RT Master Mix (Perfect Real Time) and a MJ Mini Personal Thermal Cycler (Bio-Rad Laboratories, Hercules, CA). The conditions for the reverse transcription (RT) reaction were 37°C for 15 min, whereas those for inactivation of reverse transcriptase were 85°C for 5 s. Real-time PCR analysis was then performed using SYBR Premix Ex Taq II (Tli RNaseH Plus) and a Thermal Cycler Dice Real Time System III (Takara Bio). The following real-time PCR assay protocols were used. To analyze the levels of β-actin and age-related markers such as p53, p21 and p16, the cDNA was denatured at 95°C for 30 s, followed by amplification using 55 cycles of 95°C for 5 s and 60°C for 30 s. The primer sequences used for real-time PCR analysis are shown in Table 1. mRNA levels of p53, p21 and p16 were calculated using the $2^{-\Delta\Delta Ct}$ method by normalization relative to β-actin mRNA.

Preparation of liposomal formulations. EPC or EPC/DOTAP liposomes encapsulating Asx (E/Asx-lipo or E/D/Asx-lipo, respectively) were prepared according to our previous report.[23] Briefly, a chloroform solution containing 20 mM EPC or 18 mM EPC and 2 mM DOTAP with 200 μM of Asx was dried to a thin film in a test tube using nitrogen gas. Dried lipid films were hydrated with 10% sucrose solution at room temperature and sonicated in a bath type sonicator (Bransonic, Branson Ultrasonics Corporation, Danbury, CT) to obtain a liposomal suspension of small vesicles. Finally, the liposomal suspensions were extruded using a Mini-Extruder (Avanti Polar Lipids, Alabaster, AL) with polycarbonate membrane filters (pore size 0.2 μm, Whatman, Florham Park, NJ) to sterilize and to produce liposomes having a uniform diameter. Liposomal formulations without Asx (E-lipo and E/D-lipo, respectively) were also prepared as vehicles using the same methods described above.

Evaluation of physicochemical properties of each liposomal formulation. According to our previous report, the diameters and zeta potentials of the liposomal formulations were measured using a Zetasizer Nano (Malvern Instruments, UK). The Asx concentration in each liposomal formulation was determined by dissolving 40 μl of the indicated liposomal formulation in a 2:1

Table 1. Primer sequences for real-time PCR

Gene	Forward	Reverse
p53	ACAGCGTGGTGGTACCGTAT	GGAGCTGTTGCACATGTACT
p21	ACACGCTCCCAGACGTAGTT	AGCAAAGTATGCCGTCGTCT
p16	CCAGAAGTGAAGCCAAGGAG	GTGCGGTATTTGCGGTATCT
β-actin	CCAGATCATGTTTGAGACCTTCAA	GTGGTACGACCAGAGGCATACA

chloroform:methanol mixture and adjusting the total volume to 1 ml. Calibration curve samples were also prepared at the same time by adding a known amount of Asx and EPC or EPC and DOTAP to the chloroform:methanol solvent, and adjusting the volume to 1 ml. The absorbance of the calibration curve samples and the liposomal samples were measured using a Nanophotometer, and the concentration of Asx in the liposomal formulations was calculated using an equation obtained via linear regression of the calibration curve.

Repeat-dose study using liposomal eye drops in the *in vivo* rat DED model. Liposomal Asx (E/Asx-lipo or E/D/Asx-lipo) or vehicle (E-lipo or E/D-lipo) prepared as described above were diluted with saline to prepare liposomal eye drops immediately prior to administration. Five μl of each liposomal eye drop was administered to both eyes 6 times per day for 13 days beginning on the day after surgical removal of the exorbital lacrimal glands.

Evaluation of interactions between liposomes and rat corneas. E/Asx-lipo and E/D/Asx-lipo labeled with DiI as a fluorescent lipophilic dye were prepared using the methods described above. The liposomal formulations were administered to eyes of normal rats and the eyeballs were moved 30 min later as described above. Eyeball tissue was immediately embedded in Optimal Cutting Temperature (O.C.T.) compound and frozen in an ethanol-dry ice bath. Sections of the frozen eyeball samples (20 μm thick) were prepared at –20°C with a microtome blade using a cryostat (CM3050S; Leica Biosystems Nussloch GmbH, Nussloch, Germany) and the sections were placed onto slides. Fluorescence images were obtained using a confocal laser scanning microscope (LSM700; Carl Zeiss, Jena, Germany).

Statistical analysis. All data are expressed as means ± SD. Statistical differences between groups were analyzed by one-way analysis of variance (ANOVA) followed by Dunnett's test. $P<0.05$ was considered to be statistically significant.

Results

Evaluation of tear production volume, fluorescein score and age-related marker levels in the *in vivo* rat DED model. Tear production volume of control group remained constant during the experimental period between day 0 to 25 after surgery, whereas the *in vivo* rat DED model group showed a significant decrease in the tear production volume by day 5 compared with that of the control group at day 0, and these decreased levels continued until day 25 (Fig. 2A).

The fluorescein score of the control group remained constant throughout the 25-day experimental period, indicating that these animals had no aggravation of SPK as an index symptom of corneal disorder (Fig. 2B). Meanwhile, the fluorescein score of the *in vivo* rat DED model group increased significantly after surgical removal of exorbital lacrimal glands compared with that seen for control group on day 0. The fluorescein scores for the rat DED model group continued to increase until day 15 and remained constant between days 15 and 25 (Fig. 2B, F and G).

mRNA levels of age-related markers including p53, p21 and p16 were evaluated at day 0, 15 and 25 for both the *in vivo* rat DED model and control groups. The mRNA levels of p53, p21 and p16 in the control group on days 0, 15 and 25 were similar (Fig. 2C–E), whereas the *in vivo* rat DED group showed significant up-regulation of expression on day 15 after surgery compared to values for the control group on day 0 (Fig. 2C–E). The levels of p53 and p21 mRNA in the *in vivo* rat DED model group were similar between day 15 and day 25, but the levels of p16 mRNA in this group tended to increase from day 15 to day 25 (Fig. 2C–E).

Physicochemical characteristics of liposomal formulations. We confirmed the physicochemical characteristics of liposomal formulations before applying liposomal eye drops to the *in vivo* rat DED model. The average diameters of E-lipo and E/Asx-lipo were approximately 130 nm (Table 2), whereas that for E/D-lipo and E/D/Asx-lipo were slightly smaller at approximately 80 nm (Table 2). The average polydispersity index (PDI) of all liposomal formulations was approximately 0.25, and a single peak was observed (Table 2). Liposomal formulations comprising only EPC had a mostly neutral charge, and the zeta potential for liposomal formulations composed of EPC and DOTAP showed a slight positive charge (<10 mV), which is consistent with our previous report (Table 2).[23] The actual concentration of Asx encapsulated in E/Asx-lipo and E/D/Asx-lipo was nearly equal to theoretical values at 98.6% and 101.9% for E/Asx-lipo and E/D/Asx-lipo, respectively (Table 2).

Evaluation of the effect of liposomal formulations on DED symptoms and physiochemical behaviors of *in vivo* rat DED model. We next examined how repeat-dose of each liposomal formulation prepared as eye drops that were delivered as 5 μl aliquots 6 times a day for 13 days beginning the day after surgery affected tear production volume, fluorescein score and up-regulation of age-related markers in the *in vivo* rat DED model.

As a control, saline, E-lipo or E/D-lipo lacking Asx was delivered in repeat doses to *in vivo* rat DED model and was found to have no effect on DED-mediated decreases in tear production volume, increases in fluorescein score or up-regulation of age-related markers, indicating that the liposomes themselves had no effect on DED symptoms or physiochemical behaviors (Fig. 3).

Effect of liposomal Asx having neutral charge on DED symptoms and physiochemical behaviors of *in vivo* rat DED model. Repeat-dose of liposomal formulations encapsulating 1 μM Asx that had a neutral charge, E/Asx-lipo, did not affect tear production volume (Fig. 4A), fluorescein score or up-regulation of age-related markers (Fig. 4B–E) compared to untreated *in vivo* rat DED model. However, repeat-dose of E/Asx-lipo containing 10 μM Asx did significantly suppress increases in fluorescein score compared to untreated *in vivo* rat DED model (Fig. 4B). Repeat-dose of E/Asx-lipo with 10 μM Asx also induced significant suppression of up-regulation of p53 and p16, and tended, although not significantly, to suppress p21 levels compared with untreated *in vivo* rat DED model (Fig. 4C–E).

Efficacy of positively charged liposomal Asx in the *in vivo* rat DED model. Next, repeat-dose of eye drops prepared with Asx encapsulated in positively-charged liposomes, E/D/Asx-lipo, were performed to the *in vivo* rat DED model. As seen for neutral Asx liposomes, repeat-dose of E/D/Asx-lipo carrying 0.1 to 10 μM Asx had no influence on the decreased tear production volume seen in the *in vivo* rat DED model (Fig. 5A). However, repeat-dose of E/D/Asx-lipo encapsulating >0.1 μM Asx, particularly 1 μM Asx, significantly prevented increases in fluorescein score (Fig. 5B). Compared with untreated *in vivo* rat DED model, up-regulation of p53 and p16 was significantly suppressed by repeat-dose of E/D/Asx-lipo encapsulating >0.1 μM Asx (Fig. 5C and E) whereas up-regulation of p21 tended to be suppressed by E/D/Asx-lipo with 0.1–10 μM Asx, but this effect was not significant (Fig. 5D).

These results indicate that Asx encapsulated in either neutral or positively charged liposomes does not significantly affect tear production in the *in vivo* DED model. Meanwhile, Asx does mitigate DED-mediated increases in fluorescein score and up-regulation of age-related markers when delivered as repeat-dose of eye drops containing Asx liposomal formulations. In particular, positively charged liposomes could induce these effects with lower concentrations of Asx.

Exposure levels of neutral charged and positively charged liposomes to corneas from normal rats. The results for repeat-dose of E/Asx-lipo or E/D/Asx-lipo suggested that positively-charged liposomes encapsulating Asx are more effective than neutral liposomes for prevention of DED. We observed exposure levels in normal rat corneas following administration of E/Asx-lipo or E/D/Asx-lipo labeled with the fluorescent dye

doi: 10.3164/jcbn.19-102

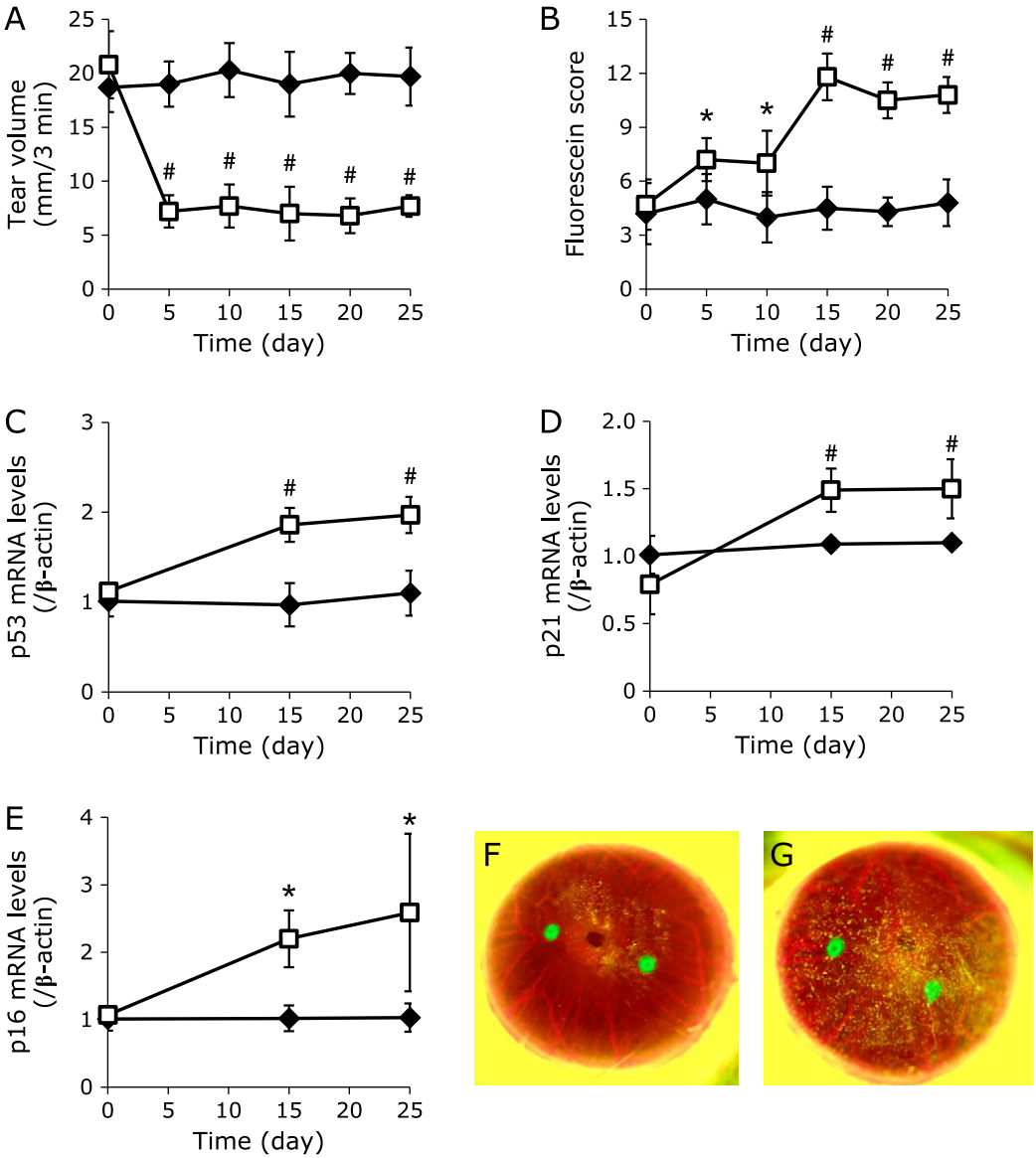

Fig. 2. Time dependence of each parameter in the *in vivo* rat DED model. Results for (A) tear volume, (B) fluorescein score, mRNA levels of (C) p53, (D) p21 and (E) p16 in the sham (◆) or the *in vivo* rat DED model (□). Data are expressed as mean ± SD ($n = 6$). *$p<0.05$, #$p<0.01$ vs the result of sham at day 0. Representative cornea photographs after fluorescein staining in (C) the sham or (D) the *in vivo* rat DED model at day 25.

Table 2. Physicochemical characteristics of each liposomal preparation

	E-lipo	E/Asx-lipo	E/D-lipo	E/D/Asx-lipo
Theoritical Asx concentration in liposomes (μM)	—	200	—	200
EPC concentration in liposome (mM)	200	200	180	180
DOTAP concentration in liposome (mM)	—	—	20	20
Particle diameter(nm)	130.3 ± 6.6	131.2 ± 7.0	75.1 ± 7.5	84.6 ± 21.1
PDI	0.209 ± 0.033	0.279 ± 0.021	0.230 ± 0.015	0.281 ± 0.086
Zeta potential (mV)	–0.88 ± 0.64	–0.39 ± 0.53	8.68 ± 0.98	8.95 ± 1.07
Actual Asx concentration in liposomes (μM)	—	197.1 ± 0.9	—	203.8 ± 3.7

PDI, polydispersity index. Data are expressed as mean ± SD ($n = 5$).

DiI to determine whether differences in the liposome formulations affected their affinity for cornea tissues. Fluorescence signals of cornea epithelia from rats treated with fluorescently-labeled E/Asx-lipo and E/D/Asx-lipo both increased 0.5 h post-administration, and were higher in the center of the cornea compared to the cornea limb (Fig. 6). Furthermore, exposure levels were higher for liposomes comprising EPC and DOTAP (i.e., positively charged) than liposomes comprising EPC only (Fig. 6). Interestingly,

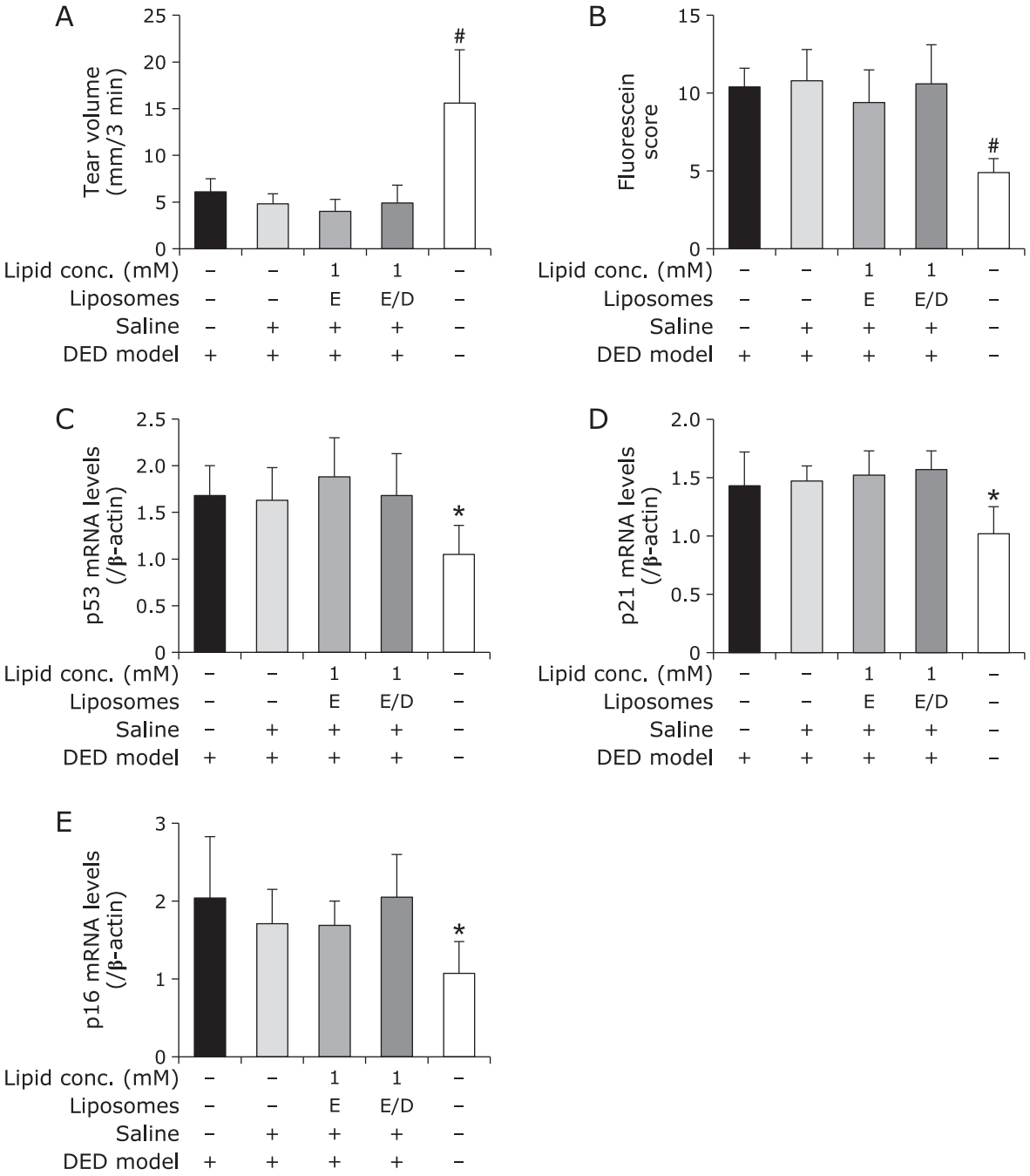

Fig. 3. Influences of repeat-dose with saline, E-lipo or E/D-lipo on each parameter in the *in vivo* rat DED model. Influence of repeat-dose with saline, E-lipo or E/D-lipo on (A) tear volume, (B) fluorescein score and mRNA levels of (C) p53, (D) p21 and (E) p16 in the *in vivo* rat DED model. Data are expressed as mean ± SD (A and B: $n = 10$, C–E: $n = 5$). *$p<0.05$, #$p<0.01$ vs *in vivo* rat DED model.

fluorescence signals were also observed in the corneal endothelium after administration of E/Asx-lipo labeled with DiI. On the other hand, administration of DiI-labeled E/D/Asx-lipo produced only low fluorescence signals in the corneal endothelium, although the fluorescence levels of the corneal epithelium treated with E/D/Asx-lipo were higher than those for E/Asx-lipo (Fig. 6). We analyzed each photograph of E/Asx-lipo and E/D/Asx-lipo using Image analysis software, Image-J (NIH) to calculate the fluorescence intensity of the corneal epithelium including Bowman's membrane, and the corneal stroma, as well as the corneal endothelium including Descemet's membrane. The fluorescence intensity ratio of the corneal epithelium, the corneal stroma and the corneal endothelium relative to the entire cornea was 79.5%, 9.5% and 11.0%, respectively, after administration of DiI-labeled E/Asx-lipo; on the other hand, for DiI-labeled E/D/Asx-lipo the relative intensities were 98.7%, 1.3% and <0.1%, respectively (Fig. 6).

Discussion

DED is a multifactorial disease, and oxidative stress induced by decreases in tear volume, excessive evaporation and hyper-

doi: 10.3164/jcbn.19-102

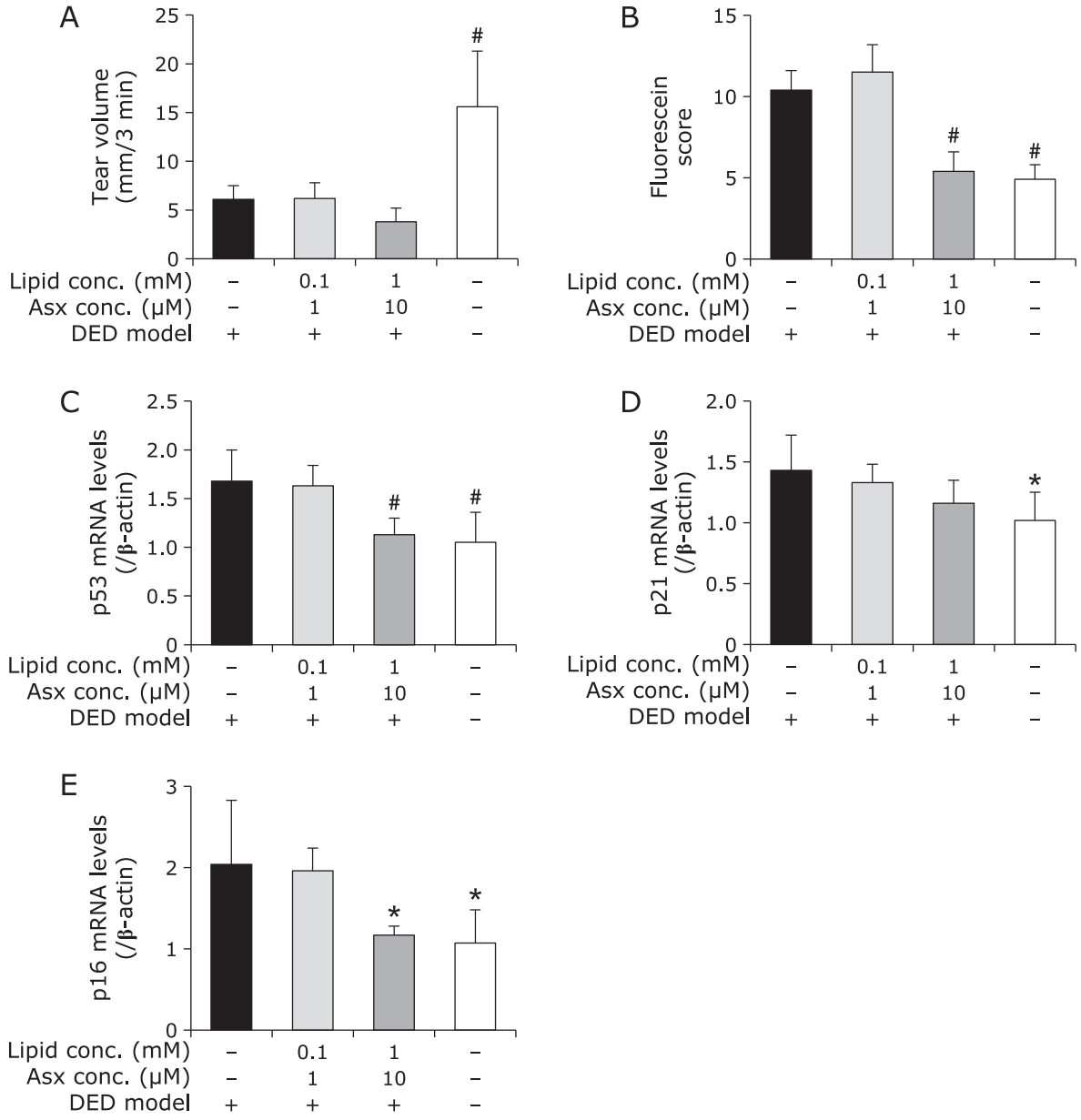

Fig. 4. Effect of repeat-administration of E/Asx-lipo on each parameter in the *in vivo* rat DED model. Effect of repeat-dose with E/Asx-lipo on (A) tear volume, (B) fluorescein score and mRNA levels of (C) p53, (D) p21 and (E) p16 in the *in vivo* rat DED model. Data are expressed as mean ± SD (A and B: n = 10–12, C–E: n = 5). *p<0.05, $^{\#}p$<0.01 vs *in vivo* rat DED model.

osmolarity of tears is a key factor in DED.[1] Previously, we reported that desiccative stress indeed results in intracellular ROS generation that is associated with up-regulated expression of age-related markers in the *in vitro* DED model, and demonstrated that Asx encapsulated in high-affinity liposomes could be a potential candidate therapeutic agent for DED.[23] In this study, we investigated the correlation between SPK as an indicator of corneal damage and expression of the age-related markers p53, p21 and p16 using the *in vivo* rat DED model. We demonstrated decreases in tear volume and up-regulated expression of p53, p21 and p16 as age-related markers, as well as increased fluorescein score as an indicator of SPK in the *in vivo* rat DED model (Fig. 2); these results were consistent with our previous report.[23]

Here we showed that repeat-dose of saline, E-lipo and E/D-lipo showed no effect on DED-related factors (Fig. 3). However, E/Asx-lipo and E/D/Asx-lipo inhibited increases in the fluorescein score and up-regulation of age-related marker expression (Fig. 4 and 5). Although repeat-dose of E/Asx-lipo and E/D/Asx-lipo had no effect on tear volume, the fluorescein score was decreased. This result suggested that Asx scavenges ROS generated by desiccative stress to suppress oxidative stress and in turn suppress increases in SPK. In the *in vivo* rat DED model, repeat-dose of liposomal formulations containing Asx indeed appeared to reduce the desiccative stress induced by decreases in tear volume and excessive tear evaporation. These results are consistent with our previous report. Also consistent with our previous results, slightly-cationic Asx liposomes showed greater efficacy than neutral Asx liposomes. Here we used confocal laser scanning microscopy to show that these slightly-cationic liposomes had higher affinity for rat corneal tissue as evidenced by higher fluorescence intensity in corneal epithelium by DiI-labeled, positively charged E/D/Asx-lipo relative to DiI-labeled neutral E/Asx-lipo (Fig. 6). Interest-

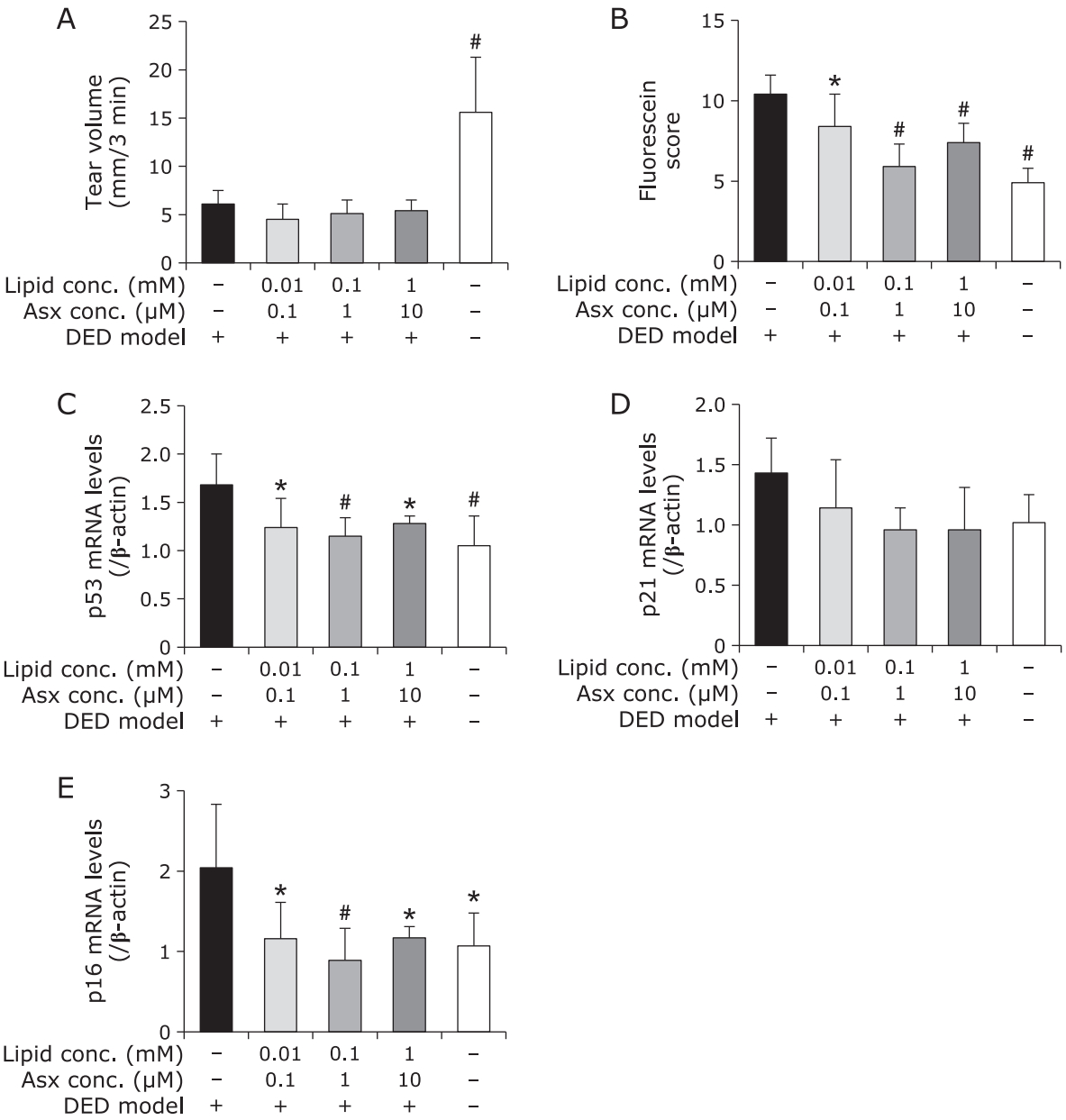

Fig. 5. Effect of repeat-dose of E/D/Asx-lipo on each parameter in the *in vivo* rat DED model. Effect of repeat-dose with E/D/Asx-lipo on (A) tear volume, (B) fluorescein score and mRNA levels of (C) p53, (D) p21 and (E) p16 in the *in vivo* rat DED model. Data are expressed as mean ± SD (A and B: n = 10–12, C–E: n = 5). *p<0.05, $^{\#}p$<0.01 vs *in vivo* rat DED model.

ingly, although the fluorescence intensity of corneal epithelium treated with E/D/Asx-lipo was higher than that treated with E/Asx-lipo, these liposomes did have a lower interaction with the corneal endothelium after administration of E/D/Asx-lipo compared with that seen for E/Asx-lipo. Cationic liposomes are known to bind to cell surfaces via electrostatic interactions.[28–30] The cornea stroma is composed of a plate layer of 60–70 collagenous fibers containing keratinocytes. Because slightly cationic charged liposomes show higher affinity for the cornea epithelium than collagenous fibers, E/D/Asx-lipo would be less likely to diffuse from the corneal epithelium to the corneal stroma, and therefore E/D/Asx-lipo would be predicted to have better antioxidative activity due to increased retention of Asx in the corneal epithelium compared to neutral E/Asx-lipo that may more readily diffuse. Thus, the characteristics of slightly cationic charged liposomes can enhance the bioavailability of eye drops that is affected by drainage systems associated with tear flow from the lacrimal gland to the nasolacrimal duct, and may also reduce the number of doses by inhibition of diffusion of an active ingredient in the corneal epithelium. This pharmaceutical formulation technology may enhance treatment compliance and improve the quality of life for DED patients.

In conclusion, we confirmed that expression of age-related markers is up-regulated in the *in vivo* rat DED model and that this up-regulation is associated with deterioration of SPK that is known to be a clinical symptom of DED. Liposomal Asx, particularly Asx encapsulated in liposomes bearing a slight positive surface charge, was effective in mitigating the negative effects of several factors associated with DED. Together our results demonstrate the potential of high affinity liposomal Asx as an effective therapeutic agent for DED.

doi: 10.3164/jcbn.19-102

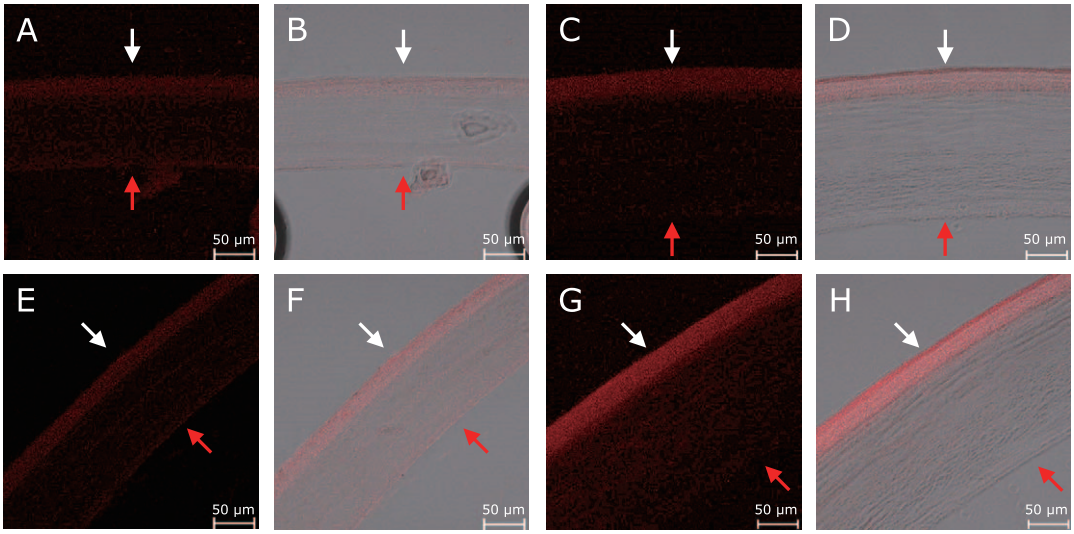

Fig. 6. Interaction of DiI-labeled E/Asx-lipo or E/D/Asx-lipo with corneal tissues. Representative fluorescence (A, C, E, G) and merged (B, D, F, H; blight and fluorescence) images of corneas from rats 0.5 h after treatment with (A–D) E/Asx-lipo or (E–H) E/D/Asx-lipo labeled with DiI. Upper and lower photographs: center and limb of corneas, respectively. White and red arrows show corneal epithelium and endothelium, respectively. Scale bars = 50 μm.

Acknowledgments

We thank all the staff members of Fuji Research Laboratories of Kowa Company, Ltd. T.F. thanks the Research Program for the Development of Intelligent Tokushima Artificial Exosome (iTEX) from Tokushima University.

Abbreviations

Asx	astaxanthin
Cdk	cyclin dependent kinase
DED	dry eye disease
DiI	1,1'-dioctadecyl-3,3,3',3'-tetramethylindocarbocyanine perchlorate
DOTAP	1,2-dioleoyl-3-trimethylammonium-propane chloride
E/Asx-lipo	liposomes encapsulating astaxanthin using egg phosphatidylcholine as lipids
E/D/Asx-lipo	liposomes encapsulating astaxanthin using egg phosphatidylcholine and 1,2-dioleoyl-3-trimethylammonium-propane chloride as lipids
E/D-lipo	liposomes using egg phosphatidylcholine and 1,2-dioleoyloxy-3-3-trimethylammonium propane chloride as lipids
E-lipo	liposomes using egg phosphatidylcholine as lipids
EPC	egg phosphatidylcholine
HCECs	human corneal epithelial cells
HEL	hexanoyl-lysine
4-HNE	4-hydroxy-2-nonenal
MDA	malondialdehyde
8-OHdG	8-hydroxy-2'-deoxyguanosine
ROS	reactive oxygen species
SPK	superficial punctate keratopathy

Conflict of Interest

The authors report no actual or potential conflict of interest, including any financial, personal or other relationships with other people or organizations within the three years that this study was conducted that could inappropriately influence, or be perceived to influence, our work.

References

1 Craig JP, Nelson JD, Azar DT, *et al*. TFOS DEWS II report executive summary. *Ocul Surf* 2017; **15**: 802–812.
2 Stapleton F, Alves M, Bunya VY, *et al*. TFOS DEW II epidemiology report. *Ocul Surf* 2017; **15**: 334–365.
3 Kawashima M, Yamada M, Suwaki K, *et al*. A clinic-based survey of clinical characteristics and practice pattern of dry eye in Japan. *Adv Ther* 2017; **34**: 732–743.
4 Deng R, Hua X, Li J, *et al*. Oxidative stress markers induced by hyperosmolarity in primary human corneal epithelial cells. *PLoS One* 2015; **10**: e0126561.
5 Nakamura S, Shibuya M, Nakashima H, *et al*. Involvement of oxidative stress on corneal epithelial alterations in a blink-suppressed dry eye. *Invest Ophthalmol Vis Sci* 2007; **48**: 1552–1558.
6 Cavet ME, Harrington KL, Vollmer TR, Wand KW, Zhang JZ. Anti-inflammatory and anti-oxidative effects of the green tea polyphenol epigallocatechin gallate in human corneal epithelial cells. *Mol Vis* 2011; **17**: 533–542.
7 Lee HS, Choi JH, Cui L, *et al*. Anti-inflammatory and antioxidative effects of *camellia japonica* on human corneal epithelial cells and experimental dry eye: *in vivo* and *in vitro* study. *Invest Ophthalmol Vis Sci* 2017; **58**: 1196–1207.
8 Higuchi A, Takahashi K, Hirashima M, Kawakita T, Tsubota K. Selenoprotein P controls oxidative stress in cornea. *Plos One* 2010; **5**: e9911.
9 Higuchi A, Inoue H, Kawakita T, Ogishima T, Tsubota K. Selenium compound protects corneal epithelium against oxidative stress. *PLos One* 2012; **7**: e45612.
10 Li Y, Liu H, Zeng W, Wei J. Edaravone protects against hyperosmolarity-induced oxidative stress and apoptosis in primary human corneal epithelial cells. *PloS One* 2017; **12**: e0174437.
11 Li Z, Choi JH, Oh HJ, Park SH, Lee JB, Yoon KC. Effects of eye drops containing mixture of omega-3 essential fatty acids and hyaluronic acid on the ocular surface in desiccation stress-induced murine dry eye. *Curr Eye Res* 2014; **39**: 871–878.
12 Foulks GN. Pharmacological management of dry eye in the elderly patients.

Drugs Aging 2008; **25**: 105–118.
13 Guillon, Maïssa C. Tear film evaporation--effect of age and gender. *Cont lenz Anterior Eye* 2010; **33**: 171–175.
14 Steven P, Braun T, Krösser S, Gehlsen U. Influence of aging on severity and anti-inflammatory treatment of experimental dry eye disease. *Klin Monbl Augenheilkd* 2017; **234**: 662–669. (in German)
15 Harper ME, Bevilacqua L, Hagopian K, Weindruch R, Ramsey JJ. Aging, oxidative stress, and mitochondrial uncoupling. *Acta Physiol Scand* 2004; **182**: 321–331.
16 Bokov A, Chaudhuri A, Richardson A. The role of oxidative damage and stress in aging. *Mech Aging Dev* 2004; **125**: 811–826.
17 Morisaki H, Ando A, Nagata Y, *et al*. Complex mechanisms underlying impaired activation of Cdk4 and Cdk2 in replicative senescence: role of p16, p21, and cyclin D1. *Exp cell Res* 1999; **253**: 503–510.
18 Stein GH, Drullinger LF, Soulard A, Dulić V. Differential roles for cyclin-dependent kinase inhibitors p21 and p16 in the mechanisms of senescence and differential in human fibroblasts. *Mol Cell Biol* 1999; **19**: 2109–2117.
19 Zhang DY, Wang HJ, Tan YZ. Wnt/β-catenin signaling induces the aging of mesenchymal stem cells through the DNA damage response and the p53/p21 pathway. *PLos One* 2011; **6**: e21397.
20 Guerin M, Huntley ME, Olaizola M. Haematococcus astaxanthin: applications for human health and nutrition. *Trends Biotechnol* 2003; **21**: 210–216.
21 Maoka T. Caritenoids in marine animals. *Mar Drugs* 2011; **9**: 278–293.
22 Aoi W, Maoka T, Abe R, Fujishita M, Tominaga K. Comparison of the effect of non-esterified and esterified astaxanthins on endurance performance in mice. *J Clin Biochem Nutr* 2018; **62**: 161–166.
23 Shimokawa T, Yoshida M, Fukuta T, Tanaka T, Inagi T, Kogure K. Efficacy of high-affinity liposomal astaxanthin on up-regulation of age-related markers induced by oxidative stress in human corneal epithelial cells. *J Clin Biochem Nutr* 2019; **64**: 27–35.
24 Koh S, Maeda N, Ikeda C, *et al*. The effect of ocular surface regularity on contrast sensitivity and straylight in dry eye. *Invest Ophthalmol Vis Sci* 2017; **58**: 2647–2651.
25 Kagawa Y, Itoh S, Shinohara H. Investigation of capsaicin-induced superficial punctate keratopathy model due to reduced tear secretion in rats. *Curr Eye Res* 2013; **38**: 729–735.
26 Kaido M, Matsumoto Y, Shigeno Y, Ishida R, Dogru M, Tsubota K. Corneal fluorescein staining correlates with visual function in dry eye patients. *Invest Opthalmol Vis Sci* 2011; **52**: 9516–9522.
27 Fujihara T, Murakami T, Fujita H, Nakamura M, Nakata K. Improvement of corneal barrier function by the P2Y(2) agonist INS365 in a rat dry eye model. *Invest Ophthalmol Vis Sci* 2001; **42**: 96–100.
28 Gao X, Huang L. Cationic liposome-mediated gene transfer. *Gene Ther* 1995; **2**: 710–722.
29 George AJ, Arancibi-Cárcamo CV, Awad HM, *et al*. Gene delivery to the corneal endothelium. *Am J Respir Crit* 2000; **162 (4 Pt 2)**: S194–S200.
30 Futaki S, Masui Y, Nakase I, *et al*. Unique features of a pH-sensitive fusogenic peptide that improves the transfection efficiency of cationic liposomes. *J Gene Med* 2005; **7**: 1450–1458.

doi: 10.3164/jcbn.19-102